Unsteady MHD convective flow of Second grade fluid through a porous medium in a Rotating parallel plate channel with temperature dependent source

M VeeraKrishna[1*] and G Subba Reddy[2]

[1]Assistant Professor, Department of Mathematics, Rayalaseema University, Kurnool, Andhra Pradesh, India.
[2]Research Scholar, Department of Mathematics, Rayalaseema University, Kurnool, Andhra Pradesh, India.

E-mail : veerakrishna_maths@yahoo.com

Abstract. We have considered the hydromagnetic convective flow of a second grade fluid through porous medium in a rotating parallel plate channel. The perturbations in the flow are created by a constant pressure gradient along the plates in addition to non-torsional oscillations of the lower plate. The analytical solutions of the velocity and the temperature are obtained using Laplace transform technique. The final steady state velocity and temperature fields are numerically discussed for different values of the governing parameters. The shear stresses and Nusselt number are put into a tabled.

Keywords. Convective flows, heat source, heat transfer, porous medium, rotating channels and unsteady state flows

1. Introduction:

The hydromagnetic rotating viscous incompressible fluid flow between parallel plates is a classical problem that has significant applications in magnetohydrodynamic (MHD) power generators and pumps, aerodynamic heating, accelerators, electrostatic precipitation polymer technology, petroleum industry, purification of crude oil and fluid droplets, sprays, designing cooling systems with liquid metal, centrifugal separation of matter from fluid and flow meters. The MHD flows of non-Newtonian fluids through porous medium are very important particularly in the fields of agricultural engineering for irrigation processes; in petroleum technology to study petroleum transport; in chemical engineering for filtration and purification processes. A series of investigations have been made by Raptis *et al*. [1-3] on the steady of two-dimensional flow past a vertical wall. Singh and Verma [4] analyzed an oscillatory three-dimensional flow through a porous medium when the permeability varied in space periodically. Singh et al. [5] investigated further a three-dimensional fluctuating flow and heat transfer through a porous medium when the permeability varied both in time and space. In view of many other important applications of MHD flows through planar channels, a number of

scholars have illustrated their interest. Notable amongst them are Shercliff [6], Ferraro and Plumpton [7], Crammer and Pai [8]. Yen and Chang [9] studied the effects of wall electrical conductance on the MHD Couette flow. A MHD flow in a duct has also been studied by Chang and Lundgren [10]. Attia and Kotb [11] investigated the two dimensional MHD flow between two porous, parallel, infinite, insulated, horizontal plates and the heat transfer through it when the lower plate was kept stationary and the upper plate was moving with uniform velocity. Singh and Mathew [12] studied the injection/suction effect on a hydro magnetic oscillatory flow in a horizontal porous channel in a rotating system. The Hall current effect on the velocity and temperature fields of an unsteady Hartmann number has also been studied by Attia [13]. Singh and Sharma [14] studied a three-dimensional Couette flow with transpiration cooling in the presence of stationary magnetic field applied perpendicular to the planes of the insulated plates. Another aspect of the above three-dimensional Couette flow when the magnetic field is fixed with the moving plate has also been investigated by Singh [15]. Mazumder, [16] studied an oscillatory Ekman boundary layer flow bounded by two horizontal plates one of which is oscillating and the other is at rest. Ganapathy [17] presented an alternative solution to the above problem. Mazumder et al., [18] analyzed the Hall effects on combined free and forced convection hydromagnetic flow through a channel. Singh [19] studied the effects of transversely applied uniform magnetic field on oscillatory flow between two parallel flat plates when the entire system rotates about an axis normal to the planes of the plates. Many researchers [20-26] have been studied on flows through different channel configurations. Recently Krishna and Prakash [27] discussed the unsteady flow of an incompressible viscous fluid in a rotating parallel plate channel bounded on one side by a porous bed under the influence of a uniform transverse magnetic field taking hall current into account. Krishna [28] discussed the unsteady flow of an incompressible electrically conducting viscous fluid in a rotating porous media. In this paper, we consider the MHD convective flow of second grade fluid through porous medium in a rotating parallel plate channel.

2. Formulation and Solution of the problem:

We consider the unsteady MHD flow of second grade fluid through porous medium bounded by two parallel non conducting plates. In undisturbed state both the plates and the fluid rotate with the same angular velocity Ω. At $t > 0$, the fluid driven by a constant pressure gradient parallel to the plate and in addition the lower plate performs non-torsional oscillation in its own plane. Further the plates are cooled or heated by a constant temperature gradient in some direction parallel to the plane at the plates.

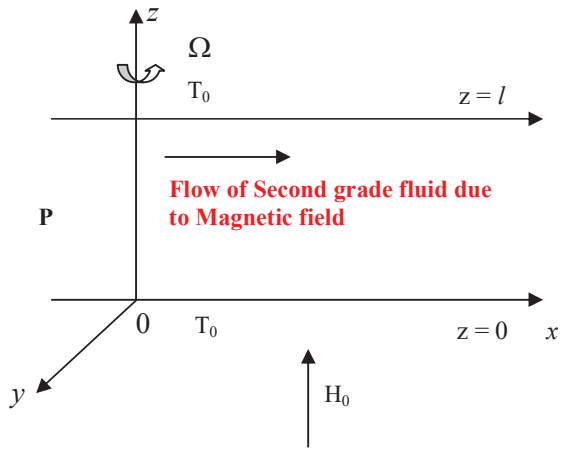

Figure 1 Physical configuration of the Problem

We choose a Cartesian co-ordinate system O(*x, y, z*) such that the plates are at $z=0$ and $z=l$ and the *z*- axis considered with the axis of rotation of the plates. The unsteady hydromagnetic boundary layer equations of motion are,

$$\frac{\partial u}{\partial t}-2\Omega v=-\frac{1}{\rho}\frac{\partial p}{\partial x}+\nu\frac{\partial^2 u}{\partial z^2}+\frac{\alpha_1}{\rho}\frac{\partial^3 u}{\partial z^2\partial t}-\frac{\sigma\mu_e^2H_0^2}{\rho}u-\frac{\nu}{k}u \tag{1}$$

$$\frac{\partial v}{\partial t}+2\Omega u=-\frac{1}{\rho}\frac{\partial p}{\partial y}+\nu\frac{\partial^2 v}{\partial z^2}+\frac{\alpha_1}{\rho}\frac{\partial^3 v}{\partial z^2\partial t}-\frac{\sigma\mu_e^2H_0^2}{\rho}v-\frac{\nu}{k}v \tag{2}$$

$$-\frac{1}{\rho}\frac{\partial p}{\partial z}-g(1-\beta(T-T_0))=0 \tag{3}$$

And the energy equation

$$\left(\frac{\partial}{\partial t}+u\frac{\partial}{\partial x}+v\frac{\partial}{\partial y}\right)(T-T_0)=\alpha_2\frac{\partial}{\partial z^2}(T-T_0)+\frac{Q}{\rho c_p}(T-T_0) \tag{4}$$

Where, *u* and *v* are dimensionless axial and transverse velocity components, ρ is the density of the fluid, μ_e is the magnetic permeability, ν is the coefficient of kinematic viscosity, *k* is the permeability of the medium, H_0 is the applied magnetic field, α_1 is the normal stress modulus, T is non- dimensional time, T_0 is the characteristic temperature, α_2 is the dimensional heat source parameter, *g* is acceleration due to gravity, β is coefficient of volume expansion, *Q* is the strength of the heat source and C_p is the specific heat at constant pressure. Since the plates widens to infinity along *x* and *y* paths, all the physical quantities except the pressure depend on z and *t* alone.

Combining equations (1) and (2), let $q= u + iv$ and therefore we obtain

$$\frac{\partial q}{\partial t}+2i\Omega q=-\frac{1}{\rho}\frac{\partial p}{\partial \xi}+\nu\frac{\partial^2 q}{\partial z^2}+\frac{\alpha_1}{\rho}\frac{\partial^3 q}{\partial z^2\partial t}-\frac{\sigma\mu_e^2H_0^2}{\rho}q-\frac{\nu}{k}q \tag{5}$$

Integrating (3) we get,

$$\frac{p}{\rho}=-gz+\beta g\int(T-T_0)\,dz+\varphi(\xi,\bar{\xi})H(t)$$

Where, $\xi=x-iy$, $\bar{\xi}=x+iy$

We use (3) in equation (5) and obtain,

$$\frac{\partial}{\partial z}\left(\frac{\partial q}{\partial t}+2i\Omega q-\nu\frac{\partial^2 q}{\partial z^2}-\frac{\alpha_1}{\rho}\frac{\partial^3 q}{\partial z^2\partial t}+\left(\frac{\sigma\mu_e^2H_0^2}{\rho}+\frac{\nu}{k}\right)q\right)=-2\beta g\frac{\partial}{\partial\xi}\left(T-T_0\right) \tag{6}$$

For the completeness of equation (6) we assume that

$$T-T_0=(Ax+By)\,H(t)+\theta_1(z,t)$$

Where *A* and *B* are the gradients of the temperature along O(*x, y*) directions respectively, $\theta_1(z, t)$ is an arbitrary function of *z* and *t*, and $H(t)$ is the Heaviside's unit step function. Taking $T_o + Ax + By + \theta_1\omega_1$ as the dimensional temperature of the lower and upper plates respectively for $t > 0$, we obtained the equation,

$$\left(\frac{\partial}{\partial t}+2i\Omega-\nu\frac{\partial^2}{\partial z^2}-\frac{\alpha_1}{\rho}\frac{\partial^3}{\partial z^2\partial t}+\frac{\sigma\mu_e^2H_0^2}{\rho}+\frac{\nu}{k}\right)q=\beta g\left(A+iB\right)zH(t)+D_1 \tag{7}$$

Where, $D_1=\frac{\partial}{\partial\xi}\left[\varphi(\xi,\bar{\xi})\right]H(t)$

The initial and boundary conditions are

$$q\left(z,t\right)=ae^{i\omega t}+be^{-i\omega t}\quad\text{at}\quad z=0 \tag{8}$$

$$q(z,t)=0 \quad \text{at} \quad z=l \quad \forall \quad t\le 0 \text{ and } \forall z \tag{9}$$

$$q(z,t)=0 \quad \text{at} \quad z=0 \quad \forall \quad t\le 0 \text{ and } \forall z \tag{10}$$

$$\theta(z,t)=\frac{\beta g l^3\left(\theta_1\omega_2-\theta_1\omega_1\right)}{\nu^2}=\theta_0 \quad \text{at} \quad z=l \tag{11}$$

Introducing the non-dimensional variables are,

$$z^*=\frac{z}{l}, q^*=\frac{ql}{\nu}, t^*=\frac{t\nu}{l^2}, \omega^*=\frac{\omega l^2}{\nu}, \theta^*=\frac{\beta g l^3\left(\theta_1-\theta_1\omega_1\right)}{\nu^2}$$

Making use of non-dimensionalization, the governing equations with respect to a rotating frame reduces to (dropping asterisks),

$$\frac{\partial^2 q}{\partial z^2}+S\frac{\partial^3 q}{\partial z^2\partial t}-\left(M^2+2iE^{-1}+D^{-2}\right)q-\frac{\partial q}{\partial t}=\mathrm{Gr}\,zH(t)+R \tag{12}$$

$$\frac{\partial^2\theta}{\partial z^2}-\alpha\theta-\mathrm{Pr}\left(\frac{\partial\theta}{\partial t}+\left(\mathrm{Gr}_1u+\mathrm{Gr}_2v\right)H(t)\right)=0 \tag{13}$$

Where, $M^2=\frac{\sigma\mu_e^2H_0^2l^2}{\rho\nu}$ the Hartmann number, $E=\frac{\nu}{\Omega l^2}$ the Ekman number, $S=\frac{\alpha_1}{\rho l^2}$ the second grade fluid parameter, $D^{-2}=\frac{l^2}{k}$ the inverse Darcy Parameter, $\mathrm{Pr}=\frac{\mu C_p}{k_1}$ the Prandtl number, $\alpha=\frac{Ql^2}{k_1}$ the Heat source Parameter, $R=\left(-\frac{l^3}{\nu^3}\right)D_1$ the Pressure gradient Parameter, $\mathrm{Gr}=\mathrm{Gr}_1+i\mathrm{Gr}_2$ the Grashof number, here, Gr_1 and Gr_2 are the Grashof numbers along *x* and *y* directions respectively.

The initial and boundary conditions are (dropping asterisks),

$$q(z,t)=ae^{i\omega t}+be^{-i\omega t} \quad \text{at} \quad z=0 \tag{14}$$

$$q(z,t)=0 \quad \text{at} \quad z=1 \quad \forall \quad t\le 0 \text{ and } \forall z \tag{15}$$

$$q(z,t)=0 \quad \text{at} \quad z=0 \quad \forall \quad t\le 0 \text{ and } \forall z \tag{16}$$

$$\theta(z,t)=\frac{\beta g l^3\left(\theta_1\omega_2-\theta_1\omega_1\right)}{\nu^2}=\theta_0 \quad \text{at} \quad z=1 \tag{17}$$

Taking Laplace transforms in the equations (12) and (13), we obtain

$$\left(1+sS\right)\frac{d^2\overline{q}}{dz^2}-\left(s+M^2+2iE^{-1}+D^{-2}\right)\overline{q}=\mathrm{Gr}\,z\,H(t)+R\,\frac{1}{s} \tag{18}$$

$$\frac{d^2\overline{\theta}}{dz^2}-\left(s\,Pr+\alpha\right)\overline{\theta}-Pr\left(\mathrm{Gr}_1u+\mathrm{Gr}_2v\right)H(t)=0 \tag{19}$$

Corresponding transformed boundary conditions,

$$\overline{q}(z,s)=\frac{a}{s-i\omega}+\frac{b}{s+i\omega} \quad \text{at} \quad z=0 \tag{20}$$

$$\overline{q}(z,s)=0 \quad \text{at} \quad z=1 \tag{21}$$

$$\overline{\theta}(z,s)=0 \quad \text{at} \quad z=0 \tag{22}$$

$$\overline{\theta}(z,s)=\frac{\beta g l^3\left(\theta_1\omega_2-\theta_1\omega_1\right)}{\nu^2}=\theta_0 \quad \text{at} \quad z=1 \tag{23}$$

We evaluate the constants involved in the transformed variables and the transformed velocity and temperature are given by

$$\bar{q} = \left(\frac{a}{s - i\omega} + \frac{b}{s + i\omega} + \frac{R}{s(1+sS)\lambda_1^2} + \frac{\mathrm{Gr}\, z}{(1+sS)\lambda_1^2} \right) \cosh \lambda_1 z +$$

$$\left\{ -\left[\frac{a}{s - i\omega} + \frac{b}{s + i\omega} + \frac{R}{s(1+sS)\lambda_1^2} + \frac{\mathrm{Gr}\, z}{(1+sS)\lambda_1^2} \right] \frac{\cosh \lambda_1}{\sinh \lambda_1} + \frac{R}{s(1+sS)\lambda_1^2 \sinh \lambda_1} \right.$$

$$\left. + \frac{\mathrm{Gr}}{(1+sS)\lambda_1^2 \sinh \lambda_1} \right\} \sinh \lambda_1 z - \frac{R}{s(1+sS)\lambda_1^2} - \frac{\mathrm{Gr}\, z}{(1+sS)\lambda_1^2} \tag{24}$$

$$\bar{\theta} = -\frac{\mathrm{Pr}\,\mathrm{Gr}}{\lambda_2^2 \mathrm{s}} \cosh \lambda_2 \mathrm{z} + \left\{ \frac{\theta_0}{\sinh \lambda_2} + \frac{\mathrm{Pr}\,\mathrm{Gr}}{\lambda_2^2 \mathrm{s}} \frac{\cosh \lambda_2}{\sinh \lambda_2} - \frac{\mathrm{Pr}\,\mathrm{Gr}}{\lambda_2^2 \mathrm{s}} \frac{1}{\sinh \lambda_2} \right\} \sinh \lambda_2 \mathrm{z} + \frac{\mathrm{Pr}\,\mathrm{Gr}}{\lambda_2^2 \mathrm{s}} \tag{25}$$

$$\text{Where, } \lambda_1^2 = \frac{s + M^2 + 2iE^{-1} + D^{-2}}{1 + sS} \text{ and } \lambda_2^2 = \mathrm{Pr}s + \alpha$$

Taking inverse Laplace transforms in the equations (24) and (25), we obtained the velocity and temperature. The shear stresses and Nusselt number are also obtained at both plates and are given by

$$\tau = \left(\frac{dq}{dz} \right)_{z=0} \text{ and } \tau = \left(\frac{dq}{dz} \right)_{z=1} ; \ \mathrm{Nu} = \left(\frac{d\theta}{dz} \right)_{z=0} \text{ and } \mathrm{Nu} = \left(\frac{d\theta}{dz} \right)_{z=1} \tag{26}$$

3. Results and Discussion:

The quasi-steady parts of the velocity and temperature representing the ultimate flow have been computed numerically for all parameters and their behaviour is plotted in Figures (2-10) for the oscillating lower plate and for plates are in rest respectively. For computational purpose we have assumed Gr to be real so that the applied pressure gradient in the *y*-direction is zero and Gr is positive or negative according as the plates are heated or cooled along the direction of the *x*-axis (non-zero pressure gradient $R = 10$, also Prandtl number Pr is chosen to be $\mathrm{Pr} = 0.71$. Figures (2-7) correspond to profiles for the velocity components *u* and *v*, Figures (8-10) correspond to profiles for temperature when one of the plates (lower) is oscillating with given amplitude and other is at rest. Tables (1-2) represent the shear stresses at the stationary and oscillatory plates while table (3) signify the rate of heat transfer at both the plates.

It is evident from the Figures (2-7) that the velocity profiles are parabolic in nature. We noticed that, the magnitudes of the velocity components *u* enhance and *v* diminish throughout the fluid region with increasing Ekman number *E* or Second grade fluid parameter *S* being the parameters fixed (Figures 2 & 5). The resultant velocity is also increases with increasing *E* and *S*. Both the velocity components *u* and *v* experiences retardation with increasing the intensity of the magnetic field (Hartmann number *M*) (Figure 3). Similar behaviour is observed for the resultant velocity. It is also noted from the Figure (4) the magnitude of the velocity component *u* diminish throughout the fluid region and the behaviour of the velocity component *v* remains the same with increasing D^{-1}. The ensuing velocity is also trim downs throughout the fluid region.

An increase in Grashof number leads to raise both *u* and *v* as shown in Figure (6). Since increase in Gr indicates supplementary heating and a reduced amount of density. The resultant velocity is also boost up throughout the fluid region. From the figure (7) depicts the velocity *u* oscillates in complete region where as *v* diminishes with increasing the frequency of oscillation ω. The ensuing velocity is also reduces with ω.

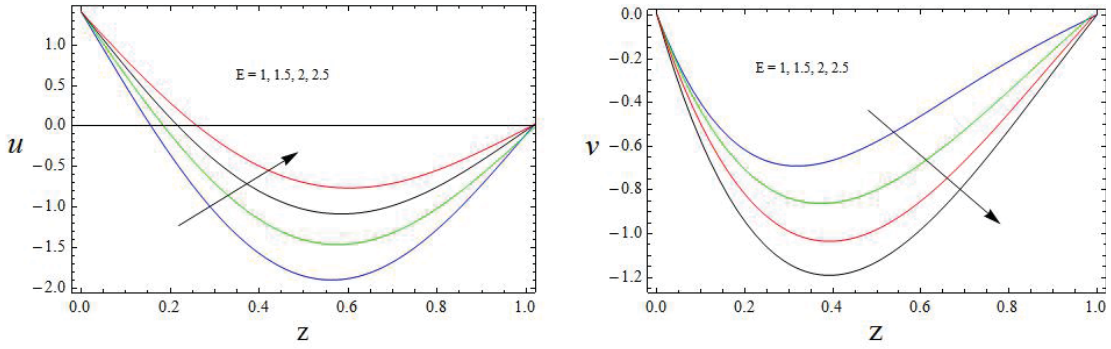

Figure 2. The velocity profiles for u and v against E
$M = 1,\ D^{-1} = 50, S = 1, \omega = \pi / 4, \mathrm{Gr} = 2$

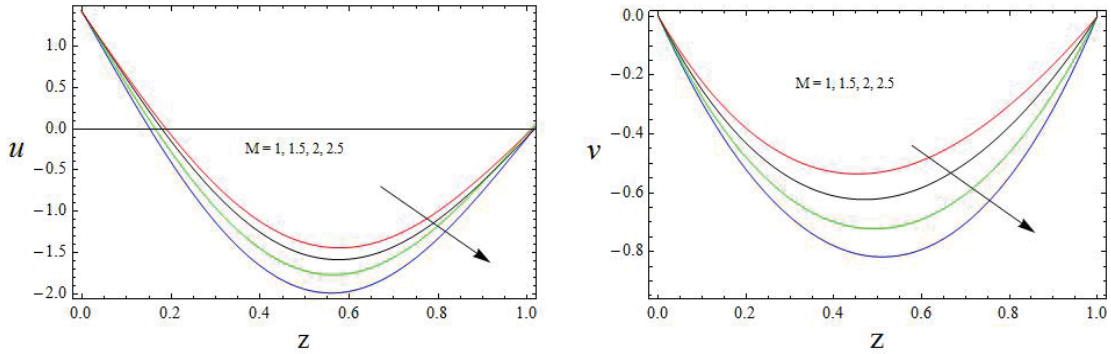

Figure 3. The velocity profiles for u and v against M
$E = 1,\ D^{-1} = 50, S = 1, \omega = \pi / 4, Gr = 2$

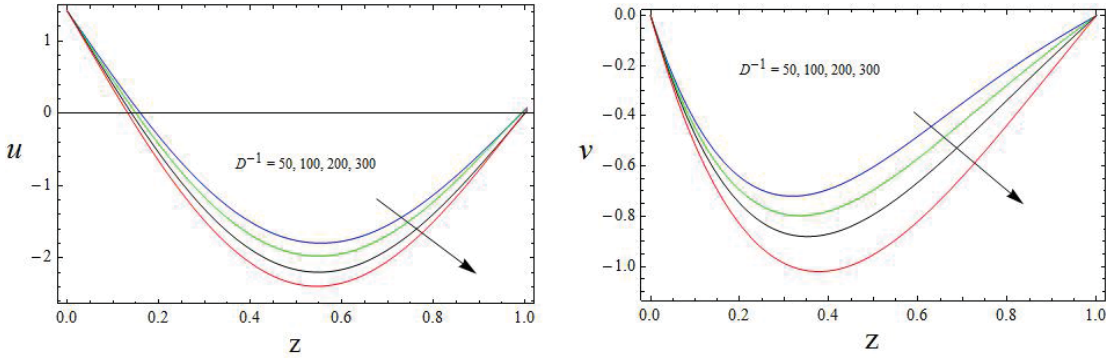

Figure 4. The velocity profiles for u and v against D^{-1}
$E = 1, M = 1, S = 1, \omega = \pi / 4,\ \mathrm{Gr} = 2$

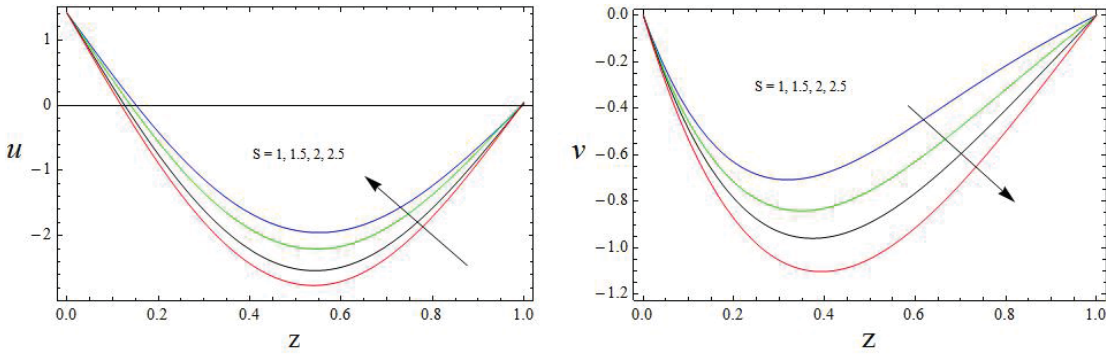

Figure 5. The velocity profiles for u and v against S
$E = 1, D^{-1} = 50, M = 1, \omega = \pi / 4, \mathrm{Gr} = 2$

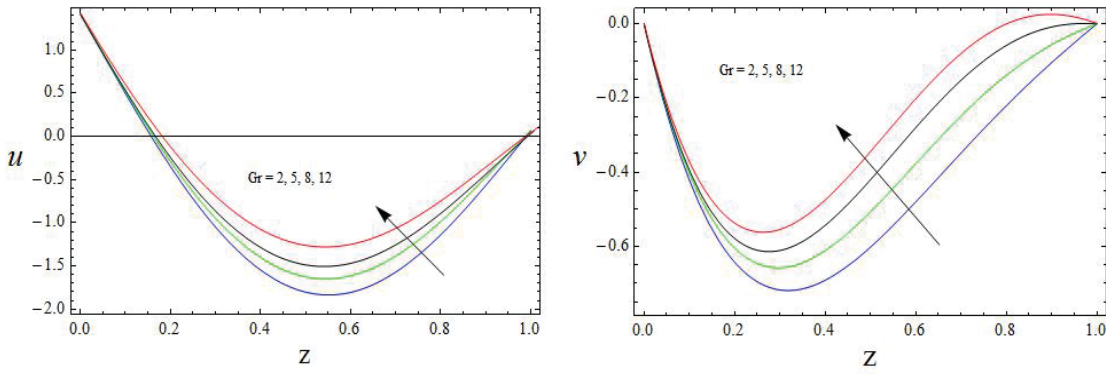

Figure 6. The velocity profiles for u and v against Gr
$E = 1, D^{-1} = 50, S = 1, \omega = \pi / 4, M = 1$

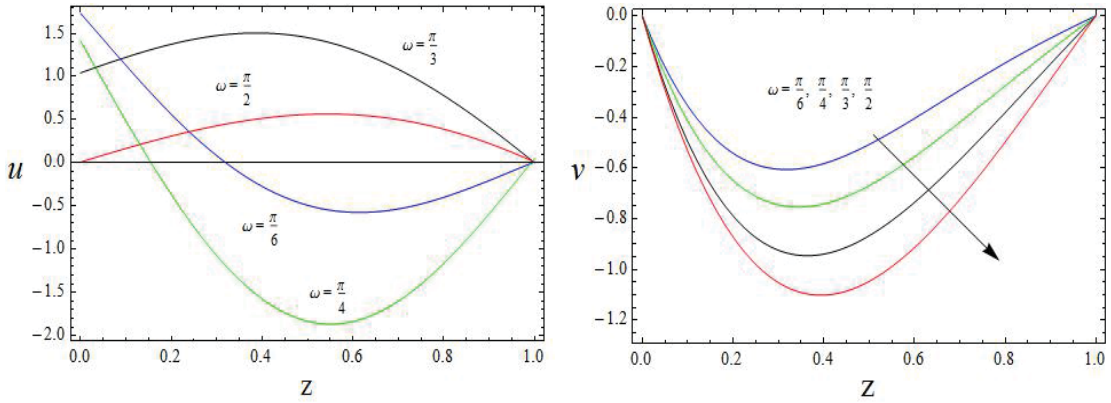

Figure 7. The velocity profiles for u and v against ω
$E = 1, D^{-1} = 50, S = 1, M = 1, Gr = 2$

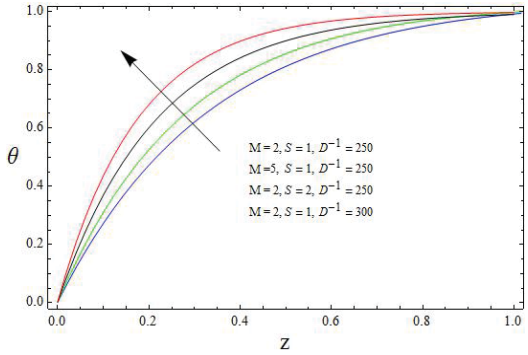

Figure 8. The Temperature Profiles for θ with M, S, and D^{-1}
$E=1, \mathrm{Gr}=2, \alpha=5, \mathrm{Pr}=0.71, \omega=\pi/4,$

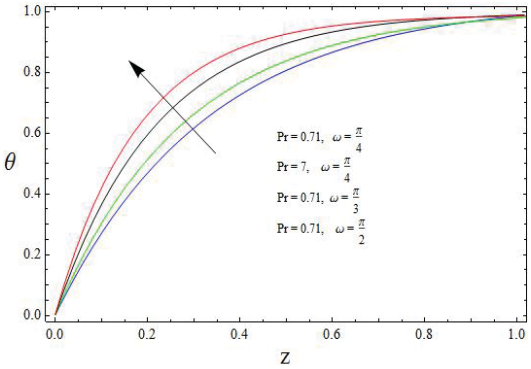

Figure 9. The Temperature Profiles for θ with Pr, and ω
$E=1, D^{-1}=250, S=1, M=1, \mathrm{Gr}=2, \alpha=5$

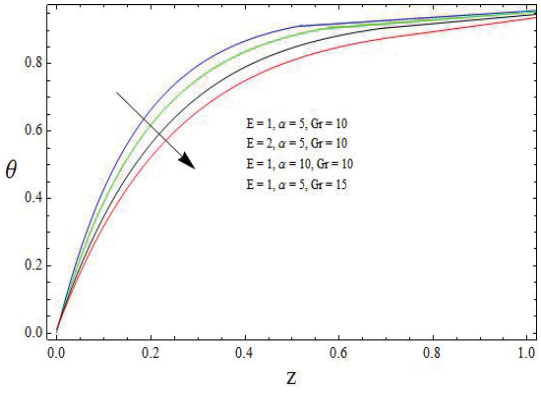

Figure 10. The Temperature Profiles for θ with E, α and Gr
$\mathrm{Pr}=0.71, D^{-1}=250, S=1, M=1, \omega=\pi/4$

Table 1. The Shear stress (τ_x & τ_y) on the stationary plate (upper plate)

E	M	D^{-1}	S	Gr	ω	τ_x	τ_y
1	**2**	**100**	**1**	**5**	$\omega = \pi / 4$	2.500285	-4.335588
1.5	2	100	1	5	$\omega = \pi / 4$	2.612425	-4.912558
2	2	100	1	5	$\omega = \pi / 4$	2.824474	-5.422851
1	**3**	100	1	5	$\omega = \pi / 4$	2.401458	-8.421847
1	**5**	100	1	5	$\omega = \pi / 4$	2.001044	-10.10854
1	2	**200**	1	5	$\omega = \pi / 4$	2.121581	-5.255547
1	2	**300**	1	5	$\omega = \pi / 4$	1.500248	-7.441522
1	2	100	**2**	5	$\omega = \pi / 4$	2.824255	-3.201254
1	2	100	**3**	5	$\omega = \pi / 4$	3.541855	-2.740116
1	2	100	1	**10**	$\omega = \pi / 4$	1.512587	-2.404152
1	2	100	1	**15**	$\omega = \pi / 4$	0.365547	-1.812279
1	2	100	1	5	$\omega = \pi / 3$	6.661485	-7.100799
1	2	100	1	5	$\omega = \pi / 2$	8.748514	-9.540548

Table 2. The Shear stress (τ_x and τ_y) on the oscillatory plate (Lower plate)

E	M	D^{-1}	S	Gr	ω	τ_x	τ_y
1	**2**	**100**	**1**	**5**	$\omega = \pi / 4$	0.640274	-0.065884
1.5	2	100	1	5	$\omega = \pi / 4$	0.795541	-0.095478
2	2	100	1	5	$\omega = \pi / 4$	0.951147	-0.225478
1	**3**	100	1	5	$\omega = \pi / 4$	0.524154	-0.096587
1	**5**	100	1	5	$\omega = \pi / 4$	0.358795	-0.147885
1	2	**200**	1	5	$\omega = \pi / 4$	0.921458	-0.086587
1	2	**300**	1	5	$\omega = \pi / 4$	1.232256	-0.095478
1	2	100	**2**	5	$\omega = \pi / 4$	1.521447	-0.196587
1	2	100	**3**	5	$\omega = \pi / 4$	2.501458	-0.854785
1	2	100	1	**10**	$\omega = \pi / 4$	0.432145	-0.112458
1	2	100	1	**15**	$\omega = \pi / 4$	0.201425	-0.501425
1	2	100	1	5	$\omega = \pi / 3$	0.688544	-0.062415
1	2	100	1	5	$\omega = \pi / 2$	0.855478	-0.030142

We notice that from the Figures (8-10) displays that the fluid temperature increases with an increase in Hartmann number M, Second grade fluid parameter S, the inverse Darcy parameter D^{-1}, Prandtl number Pr, and the frequency of oscillation ω. The temperature reduces with increasing Ekman number E, Heat source parameter α and Grashof number Gr.

The shear stresses (τ_x & τ_y) and Nusselt number (Nu) are calculated computationally at the stationary and oscillatory plates and tabulated on the tables (1-3). At the stationary plate, τ_x and τ_y boosts with increasing Ekman number E, and the frequency of oscillation ω. The reversal behavior is observed for increasing Grashof number Gr. The stresses τ_x reduce and τ_y increase in magnitude with M or D^{-1}, whereas stresses τ_x increases and τ_y decreases with increasing second grade fluid parameter S (Table 1). At the oscillatory plate, τ_x and τ_y improved with increasing E, D^{-1} and S. The stresses τ_x reduce and τ_y increase in magnitude with increasing M or Gr. The reversal behavior is observed for increasing ω (Table 2).

The magnitudes of the rate heat transfer Nu enhance with increasing Ekman number E, inverse Darcy parameter D^{-1}, Grashof number Gr, the frequency of oscillation ω and Prandtl number Pr at either plates. The Nusselt number increases at stationary plate and reduces at oscillatory plate with increasing second grade fluid parameter S, where as reversal trend observed with increasing M or Heat source parameter α (Table 3).

Table 3. The Rate of Heat transfer (Nusselt number) at stationary plate and oscillatory plate

E	M	D^{-1}	S	Gr	ω	α	Pr	stationary plate	oscillatory plate
1	**2**	**100**	**1**	**5**	$\omega = \pi / 4$	**5**	**0.71**	1.541255	3.421457
1.5	2	100	1	5	$\omega = \pi / 4$	5	0.71	2.501241	5.614255
2	2	100	1	5	$\omega = \pi / 4$	5	0.71	3.201425	6.924157
1	**3**	100	1	5	$\omega = \pi / 4$	5	0.71	1.202251	4.841657
1	**5**	100	1	5	$\omega = \pi / 4$	5	0.71	0.814785	6.404874
1	2	**200**	1	5	$\omega = \pi / 4$	5	0.71	2.841552	2.414248
1	2	**300**	1	5	$\omega = \pi / 4$	5	0.71	3.966358	2.000475
1	2	100	**2**	5	$\omega = \pi / 4$	5	0.71	1.868547	2.814148
1	2	100	**3**	5	$\omega = \pi / 4$	5	0.71	2.144445	2.213485
1	2	100	1	**10**	$\omega = \pi / 4$	5	0.71	5.750548	9.855478
1	2	100	1	**15**	$\omega = \pi / 4$	5	0.71	8.400485	15.14748
1	2	100	1	5	$\omega = \pi / 3$	5	0.71	1.996588	5.601825
1	2	100	1	5	$\omega = \pi / 2$	5	0.71	2.601495	8.001625
1	2	100	1	5	$\omega = \pi / 4$	**8**	0.71	1.221485	8.752466
1	2	100	1	5	$\omega = \pi / 4$	**10**	0.71	0.007088	13.65246
1	2	100	1	5	$\omega = \pi / 4$	5	**7**	2.821479	8.225478

4. Conclusions:

We have considered MHD convective flow of second grade fluid through a porous medium in a rotating parallel plate channel. The important findings are,

1. The resultant velocity is increases with increasing E and S, also trim downs throughout the fluid region with increasing M, ω or D^{-1}.
2. Both velocities are raised with Gr.
3. The fluid temperature increases with an increase in M, S, D^{-1}, Pr and ω.
4. The temperature reduces with increasing E, α and Gr.
5. The magnitude of the both stresses enhances with increasing E and ω, also reduces for increasing Gr at the stationary plate.
6. The magnitude of the both stresses enhances with increasing E, D^{-1} and S at the oscillatory plate. The stresses reduce in magnitude with increasing M, Gr or ω.
7. The magnitudes of the rate heat transfer (Nu) enhance with increasing E, D^{-1}, Gr, ω and Pr at either plates. Nu increases at stationary plate and reduces at oscillatory plate with increasing S, where as reversal trend observed with increasing M or α.

References:

[1]. Raptis A Perdikis C and Tzivanidis G 1981 Free Convection Flow through a Porous Medium Bounded by a Vertical Surface *Journal of Physics D: Applied Physics*, 14, 99-102.
[2]. Raptis A Tzivanidis G and Kafousias N 1981 Free Convection and Mass Transfer Flow through a Porous Medium Bounded by an Infinite Vertical Limiting Surface with Constant Suction *Letters Heat Mass Transfer*, 8, 417-424.
[3]. Raptis A Kafousias N and Massalas C 1982 Free Convection and Mass Transfer Flow through a Porous Medium Bounded by an Infinite Vertical Porous Plate with Constant Heat Flux *Zeitschrift für Angewandte Mathematik und Mechanik*, 62, 489-491.
[4]. Singh K D and Verma G N 1995 Three-Dimensional Oscillatory Flow through a Porous Medium with Periodic Permeability *Zeitschrift für Angewandte Mathematik und Mechanik*, 75, 599-604.
[5]. Singh K D Sharma R and Chand K 2000 Three-Dimensional Fluctuating Flow and Heat Transfer through a Porous Medium with Variable Permeability *Zeitschrift für Angewandte Mathematik und Mechanik*, 80, 473-480.
[6]. Shercliff T A 1965 A Text-Book of Magneto Hydro Dynamics *Pergamon Press*, London.
[7]. Ferraro V C A and Plumpton C 1966 An Introduction to Magneto Fluid Mechanics *Clarandon Press*, Oxford.
[8]. Crammer K P and Pai S I 1973 Magneto Fluid Dynamics for Engineers and Applied Physicist *McGraw Hill Book Co.*, New York.
[9]. Yan J T and Chang C C 1964 Magneto Hydrodynamic Couette Flow as Affected by Wall Electrical Conductance *Zeitschrift für Angewandte Mathematik und Physik*, 15, 400-407.
[10]. Chang C C and Lundgren T S 1961 Duct Flow in Magneto Hydrodynamics *Zeitschrift für Angewandte Mathematik und Physik*, 12, 100-114.
[11]. Attia H A and Kotb N A 1996 MHD Flow between Two Parallel Plates with Heat Transfer *Acta Mechanica*, 117, 215-220.
[12]. Singh K D and Alphonsa M 2008 Injection/Suction Effects on an Oscillatory Hydromagnetic Flow in a Rotating Horizontal Porous Channel *Indian Journal of Physics*, 82, 435-445.
[13]. Attia H A 2006 Time Varying Hydro Magnetic Couette Flow with Heat Transfer of a Dusty Fluid in the Presence of Uniform Suction and Injection Considering the Hall Effect *Turkish Journal of Engineering and Environmental Sciences*, 30, 285-297.
[14]. Singh K D and Rakesh S 2001 MHD Three-Dimensional Couette Flow with Transpiration Cooling *Zeitschrift für Angewandte Mathematik und Mechanik*, 81, 715-720.
[15]. Singh K D 2004 Influence of Moving Magnetic Field on Three-Dimensional Couette Flow *Zeitschrift für Angewandte Mathematik und Physik*, 55, 894-902.
[16]. Mazumder B S 1991 An Exact Solution of Oscillatory Couette Flow in a Rotating System *Journal of Applied Mechanics*, 58, 1104-1107.
[17]. Ganapathy R A 1994 A Note on Oscillatory Couette Flow in a Rotating System *Journal of Applied Mechanics*, 61, 208-209.
[18]. Mazumder B S Gupta A S and Datta N 1976 Hall Effects on Combined Free and Forced Convective Hydromagnetic Flow through a Channel *International Journal of Engineering Science*, 14, 285-292.
[19]. Singh K D 2000 An Oscillatory Hydromagnetic Couette Flow in a Rotating System *Zeitschrift für Angewandte Mathematik und Mechanik*, 80, 429-432.
[20]. Hartmann J and Lazarus F 1937 Kongelige danske videnskabernes selskab *Matematisk-Fysiske Meddelelser*, 15, 6-7.
[21]. Debnath L Ray S C and Chatterjee A K 1979 Effects of Hall Current on Unsteady Hydromagnetic Flow past a Porous Plate in a Rotating Fluid System *Zeitschrift für Angewandte Mathematik und Mechanik*, 59, 469-471.

[22]. Prasada Rao D R V and Krishna D V 1981 Hall Effect on Unsteady Hydromagnetic Flow *Indian Journal of Pure and Applied Mathematics*, 12, 270-276.
[23]. Prasada Rao D R V Krishna D V and Debnath L 1982 Hall Effects on Free and Forced Convective Flow in a Rotating Channel *Acta Mechanica*, 43, 49-59.
[24]. Veera Krishna M and Suneetha S V 2009 Hall Effects on Unsteady MHD Rotating Flow of an Incompressible Viscous Fluid through a Porous Medium *Journal of Pure and Applied Physics*, 21, 143-156.
[25]. Suneetha S V Veera Krishna M and Siva Pradad R 2010 Hall Effect on Unsteady Rotating Hydro Dynamic Flow of an Incompressible Second Grade Fluid in a Porous Half Space *Journal of Pure and Applied Physics*, 22, 143-156.
[26]. Das S Mandal H K and Jana R N 2013 Hall Effect on Unsteady MHD Flow through a Porous Channel in a Rotating System with Variable Pressure Gradient *Ph.D. Thesis, Vidya Sagar University, Midnapur*, 1-23.
[27]. M VeeraKrishna and J Prakash 2015 Hall Current Effects on Unsteady MHD Flow in a Rotating Parallel Plate Channel Bounded by Porous Bed on the Lower Half-Darcy Lapwood Model *Open Journal of Fluid Dynamics*, 5, 275-294. http://dx.doi.org/10.4236/ojfd.2015.54029
[28]. M.VeeraKrishna 2016 Unsteady MHD Flow in a Rotating Parallel Plate Channel under the Influence of Pressure Gradient with Hall Current Effects *Journal of Scientific Research and Reports*, 10(3), 1-21. http://dx.doi.org/10.9734/JSRR/2016/24123.